Journal of Protein Chemistry, Vol. 22, No. 2, February 2003 (© 2003)

Combinatorial Evolution of High-Affinity Peptides that Bind to the Thomsen-Friedenreich Carcinoma Antigen

Linda A. Landon,[1] Elena N. Peletskaya,[2] Vladislav V. Glinsky,[1] Natalia Karasseva,[3] Thomas P. Quinn,[1] and Susan L. Deutscher[1,4,5]

Received December 13, 2002

Thomsen-Friedenreich (TF) antigen occurs on approximately 90% of human carcinomas, is likely involved in carcinoma cell homotypic aggregation, and has clinical value as a prognostic indicator and marker of metastasized cells. Previously, we isolated anti-TF antigen peptides from bacteriophage display libraries. These bound to TF antigen on carcinoma cells but were of low affinity and solubility. We hypothesized that peptide amino acid sequence changes would result in increased affinity and solubility, which would translate into improved carcinoma cell binding and increased inhibition of aggregation. The new peptides were more soluble and exhibited up to fivefold increase in affinity ($K_d \cong 60$ nM). They bound cultured human breast and prostate carcinoma cells at low concentrations, whereas the earlier peptides did not. Moreover, the new peptides were potent inhibitors of homotypic aggregation. The maturated peptides will have expanded applications in basic studies of the TF antigen and particular utility as clinical carcinoma-targeting agents.

KEY WORDS: Bacteriophage display; affinity maturation; carcinoma antigen; peptide; glycoepitope; fluorescence quenching; confocal microscopy.

1. INTRODUCTION

Tumorigenic transformation of mammalian cells results in changes in the repertoire of cell surface carbohydrates (Brockhausen *et al.*, 1998) and can lead to pathologic alterations in cellular adhesion and motility functions (Matarrese *et al.*, 2000). Numerous studies in cultured cell systems, which have been derived from a variety of human cancers, indicate that changes in the cell surface expression of molecules that are involved in adhesion promote carcinoma cell aggregation and increase the efficiency of metastasis in mouse tumor models (Li *et al.*, 2001; Updyke and Nicolson, 1986; Yakushijin *et al.*, 1998). The carcinoma cell–associated carbohydrate antigen, the Thomsen-Friedenreich (TF)[6] antigen, may participate in both physiological and pathological processes that involve cell adhesion (Glinsky *et al.*, 2000, 2001; Matarrese *et al.*, 2000) and migration (Matarrese *et al.*, 2000). Springer and colleagues demonstrated that polyagglutination in aging red blood cells and carcinoma cell homotypic aggregation were both caused by interactions

[1] Department of Biochemistry, M121 Medical Sciences Bldg., University of Missouri, Columbia, Missouri 65212.
[2] National Cancer Institute-FCRDC, HIV Drug Resistance Program, P.O. Box B, Bldg. 539, Room 104, Frederick, Maryland 21702-1201.
[3] Department of Health Professions, E102, Vet. Med. Bldg., University of Missouri, Columbia, Missouri 65211.
[4] Harry S Truman Memorial Veterans Administration Hospital, Research Service, 800 Hospital Dr., Columbia, Missouri 65201-5297.
[5] To whom correspondence should be addressed. E-mail: deutschers@missouri.edu

[6] Abbreviations: ASF, asialofetuin; AU, arbitrary units; B_{max}, maximal binding; BSA, bovine serum albumin; CM-DPBS, Ca^{2+}- and Mg^{2+}-free Dulbecco's PBS; cpm, counts per minute; EC_{50}, half-maximal effective concentration; EDTA, disodium ethylenediaminetetraacetate; FITC, fluoroscein isothiocyanate; HSA, human serum albumin; K_d, dissociation constant; MPFI, mean pixel fluorescence intensity; MPI, mean pixel intensity; MAP, multiple antigen peptide; NNK, N = any deoxynucleotide and K = equal mixture of G and T; pI, isoelectric point; PNA, *Arachis hypogaea* lectin; Q_{max}, maximum fluorescence; Q_{obs}, observed fluorescence; PBS, phosphate-buffered saline; RT, room temperature; SA-AP, streptavidin–alkaline phosphatase conjugate; Sialyl-LACNAc, sialyl-galactose β 1→4 *N*-acetylglucoseamine; TF, Thomsen-Friedenreich; TTBS, Tween-Tris–buffered saline. The universal one-letter codes for amino acids are used.

0277-8033/03/0200-0193/0 © 2003 Plenum Publishing Corporation

between a blood group–related disaccharide, later identified as the TF antigen, and cell surface proteins that specifically bound to the TF antigen (Springer *et al.,* 1975, 1983; Springer and Desai, 1977). The TF antigen has been used clinically as a prognostic indicator (Baldus *et al.,* 2000) and as a marker of metastasized carcinoma cells (Baldus *et al.,* 1998).

The TF antigen (galactose β1→3 *N*-acetyl-galactosamine) (Peletskaya *et al.,* 1996, 1997) occurs on up to 90% of human carcinomas (Springer, 1984). In normal cells, the TF antigen is a sialylated, *O*-linked core oligosaccharide structure found on cell surface and secreted glycoproteins (Baldus *et al.,* 1998, 2000; Brockhausen *et al.,* 1998). In carcinoma cells, however, the TF antigen occurs in its immature, nonsialylated form (Brockhausen *et al.,* 1998). Although the concentration of the desialylated TF antigen in healthy tissues is quite low (Cao *et al.,* 1996), several lines of evidence indicate that the TF antigen concentration is markedly increased in carcinoma. The naturally occurring anti-TF antigen serum agglutinin titer is reduced in carcinoma patients (Springer and Desai, 1977), and there is increased binding of TF antigen-binding lectins and antibodies to tumor relative to normal tissue (Springer *et al.,* 1975).

Because of the physiological and clinical relevance of the TF antigen, small, high-affinity anti-TF antigen molecules (Lundquist *et al.,* 2000) would have wide applicability as tumor cell–targeting agents and may further discern the role of the TF antigen in various processes, such as cell adhesion and cancer metastasis. However, most high-affinity carbohydrate binding molecules are larger multivalent molecules (Lundquist *et al.,* 2000) with physicochemical characteristics that limit their clinical and basic science applications (Jain, 1989). Previously, our laboratory identified a series of small peptides that bound to the TF antigen, which were selected from a combinatorial library of random 15 amino acid peptides that was displayed on the surface of bacteriophage. A TF antigen–binding amino acid consensus sequence was identified (W-Y-A-W/F-S-P) (Peletskaya *et al.,* 1996, 1997). The first-generation peptides, including P30 (HGRFILP-WWYAF SPS) (Peletskaya *et al.,* 1996), bound to the TF antigen on selected cultured human carcinoma cell lines and interfered with metastasis-related cell aggregation events (Glinsky *et al.,* 2000, 2001; Peletskaya *et al.,* 1997). Although these results indicated that the peptides were targeting the TF antigen and had antiaggregation potential, the peptides exhibited low monomeric affinity for the TF antigen and could not be dissolved at high concentration in aqueous buffers, which significantly limited their use.

Thus, a new generation of anti-TF antigen peptides were sought. Specifically, we wished to identify peptides with enhanced carcinoma cell–targeting ability, potent antiaggregation functions, and increased solubility. We hypothesized that changes to the peptide amino acid sequence would result in increased affinity and solubility, which would translate into improved carcinoma cell–binding characteristics and increased potency of inhibition of aggregation.

In this study, improved peptide sequences were identified by using a targeted combinatorial search of the sequence space immediately surrounding the TF antigen–binding consensus sequence to identify amino acid sequences with maturated function. A library of peptides was designed, in which the six-residue TF antigen–binding consensus sequence was held constant and was flanked on each side by domains of random four- or five-amino-acid sequences. To select maturated anti-TF antigen peptides, the peptide library was displayed on bacteriophage and affinity selected against purified TF antigen–bearing glycoproteins.

Combinatorial maturation is a powerful chemical tool to use to improve the binding affinity or other function of novel targeting agents for clinically or biochemically relevant antigens. Theoretically, combinatorial maturation compensates for the sparse representation in the initial combinatorial library of sequences related to the optimum sequence and increases the probability of finding rare mutations that improve upon protein function (Scott and Smith, 1990; Yu and Smith, 1996). Studies in T cell receptors and antibodies clearly indicate that targeted combinatorial techniques can break the "affinity ceiling" and improve antibody function (Foote and Eisen, 2000). Yelton *et al.* (1995) reported affinity maturation of an antibody that recognizes Lewis Y-type carbohydrates, but maturation of affinity in small carbohydrate binding molecules has not been reported.

Combinatorial maturation yielded second-generation peptides that bound to the TF antigen with improved affinity and that also exhibited superior binding to the surfaces of cultured human breast (MDA-MB-435) and prostate (DU 145, LNCaP) carcinoma cell lines displaying the TF antigen. Moreover, the second-generation peptides were potent inhibitors of metastasis-related homotypic aggregation of cultured carcinoma cells. These results supported our hypothesis that combinatorial maturation could improve upon the carcinoma targeting and metastasis-related antiaggregation functions of carbohydrate binding peptides. To the best of our knowledge, this is the first example of the maturation of carbohydrate binding affinity and an antiadhesion function in a soluble peptide ligand. The second-generation peptides, which are described herein, will have important applications in further experiments to define the physiological and patho-

logical roles of the TF antigen and may serve as diagnostic and therapeutic agents in the treatment of many forms of carcinoma.

2. MATERIALS AND METHODS

2.1. Materials

Unless specifically noted, all reagents were purchased from Sigma Chemical Co. (St. Louis, MO). Commercial ASF was prepared from fetuin by enzymatic removal of the terminal sialic acid groups that masked fetuin's 3 sialyl-TF antigen disaccharides (Edge and Spiro, 1987). The fUSE5 vector was kindly provided by Dr. George P. Smith (Scott and Smith, 1990).

2.2. fUSE5 Bacteriophage Microlibrary Construction

A library of double-stranded DNA oligonucleotide cassettes was synthesized commercially (Sigma-Genosys, Inc., Woodlands, TX). The plus-strand sequence was 5′-TCG GCC GAC GGG GCC $(NNK)_5$ TGG TAT GCG TGG TCC CCG $(NNK)_4$ GGG GCC TCT GGG GCC GAA AGT-3′, where K represented an equal mixture of G and T, and N represented an equal mixture of all four deoxynucleotides. NNK represented an equal mixture of 32 triplet codons, including codons for all 20 amino acids and the amber stop codon (3′-UAG-5′). The resulting peptides contained the six-amino-acid TF antigen–binding consensus sequence (W-Y-A-W/F-S-P) (Peletskaya *et al.*, 1996, 1997) in the conserved central part of the peptide and terminal regions of random amino acid sequence. The large size of the input library (10^{11} bacteriophage particles) indicated that a large percentage of the possible 15-amino-acid peptides were represented in the library (Scott and Smith, 1990).

To construct the bacteriophage vector, the oligonucleotide cassettes were digested with *Bgl*II and ligated (10-fold molar excess) into the fUSE5 vector (40 μg total), which was linearized by *Sfi*I endonuclease digestion. The fUSE5 vector (Scott and Smith, 1990) encodes for a library of bacteriophages, each displaying one or more copies of the recombinant peptide, with unique primary sequence, in the context of the pIII coat protein. The ligation reaction was conducted overnight at 16°C in 30 mM Tris-HCl, pH 7.5, 30 mM NaCl, 7.4 mM $MgCl_2$, 2 mM dithioerythritol, 0.2 mM disodium ethylenediaminetetraacetate (EDTA), 1 mM spermidine, 0.1 mg/ml acetylated bovine serum albumin (BSA), and 0.25 M ATP. The ligation product was used to transform Library Efficiency DH5α-F′ competent cells (Life Technologies, Rockville, MD) and inoculate 6 L of terrific broth (1.2% bactotryptone, 2.4% yeast extract, 0.504% glycerol, 8.9 mM potassium phosphate, and 10 μg/ml tetracycline). Transformation efficiency was estimated by serial dilutions of the transformation culture. The transformation yield was estimated to be 8×10^9 transforming units.

2.3. Affinity Selection

For three rounds of selection, the TF antigen conjugated to human serum albumin (HSA) was immobilized on a streptavidin-coated Petri dish. Bacteriophage particles were allowed to bind for 4 hr on a rocker table at 4°C. After extensive washing, bound bacteriophage particles were eluted with 400 μl of 0.1 N HCl, pH 2.2, 1 mg/ml BSA and were titered. Colonies from the final-round output titering plates were used as individual output clones. Bacteriophage clones were selected for sequencing based upon the intensity of their signal on a bacteriophage membrane binding assay, as described previously (Peletskaya *et al.*, 1996). The inserts from 196 clones from the combined output of the final round were sequenced to identify the encoded peptides, by using a modified dideoxy sequencing method, as described previously (Peletskaya *et al.*, 1997).

2.4. Peptide Sequence Analysis and Synthesis

Peptide sequence analysis was performed by using the ALIGN and FASTA programs and the GCG (Genetics Computer Group, Inc., Madison, WI) software package. Peptides were synthesized by using an Advanced ChemTech 396 multiple peptide synthesizer (Advanced ChemTech, Louisville, KY) and solid-phase Fmoc chemistry. Peptides were purified by using high-pressure liquid chromatography. Their masses were verified by using mass spectroscopy.

2.5. Peptide Binding to Immobilized ASF

The 1-μl aliquots of 1 mM ASF were spotted onto a nitrocellulose membrane and dried. The nitrocellulose was blocked (10 mM Tris, pH 7.5, 6% BSA) and washed with Tris-buffered saline, pH 7.5, 0.1% Tween (TTBS). The nitrocellulose was incubated with peptide solutions (100 μM in 10 mM Tris, pH 7.5, 6% BSA) for 1 hr, washed, blocked, and then incubated with streptavidin–alkaline phosphatase conjugate (SA-AP) for 1 hr. Peptide binding was detected colorimetrically by using nitro

blue tetrazolium, 5-bromo-4-chloro-3-indolyl phosphate, and *p*-toluidine salt in substrate buffer (50 mM Tris, pH 9.5, 50 mM NaCl, 2.5 mM $MgCl \cdot 6H_2O$). The dot blots were dried and immediately scanned to create a digital image. The mean pixel intensity (MPI) of the colored dot was obtained from nonmanipulated scans by using the Adobe Photoshop software package "Histogram" function, which derived the MPI by calculating the average pixel intensity for the selected pixels. Adobe Photoshop reported MPI in arbitrary units (AU) (Miller *et al.*, 1997). The MPI value of the SA-AP–only dot blot was subtracted from all peptide MPI values before analysis. The MPI of P30 was designated as basal MPI (MPI = 1). Percent change from basal MPI was calculated by using the Microsoft Excel software package and the formula: Percent increase = $[(MPI^{\text{second-generation peptide}} - MPI^{P30})/MPI^{P30}] * 100$.

2.6. Fluorescence Quenching

Fluorescence quenching was used to study the binding affinity of the anti-TF antigen peptides for the TF antigen. The fluorophore molecule AlexaFluor 488 was conjugated to ASF or other glycoproteins, according to the manufacturer's directions (AlexaFluor 488 labeling kit; Molecular Probes, Eugene, OR). When the peptides bound to the carbohydrates on the labeled glycoproteins, the fluorescence of AlexaFluor 488 was quenched, likely because of interactions between the fluorophore and tryptophan residues in the peptides (Mummert and Voss, 1996).

Fluorescence quenching was conducted exactly as described previously (Komissarov *et al.*, 1996, 1997; Peletskaya *et al.*, 1997) except that AlexaFluor 488 was used as a fluorophore rather than fluoroscein isothiocyanate (FITC). AlexaFluor 488 is superior to FITC for fluorescence quenching studies because it has a higher fluorescent yield, its fluorescence is not affected by buffer pH, and it is less sensitive to photobleaching (Panchuk-Voloshina *et al.*, 1999). Emission spectra were obtained over the wavelengths 500–550 nm. Titrations (495-nm excitation, 519-nm emission) were conducted by adding increasing concentrations of peptides into a 1 nM fluorophore solution (10 mM Tris, pH 7.5). Following equilibration, fluorescence emission in counts per minute (cpm) was recorded. For titrations, maximum fluorescence (Q_{max}) was defined as the fluorescence at 519 nm of the unliganded fluorophore, and observed fluorescence (Q_{obs}) was defined as the fluorescence at 519 nm of the liganded fluorophore. Each reported Q_{max} and Q_{obs} value was the average of readings from a 10-s period and was corrected for photobleaching (Kim *et al.*, 1994). Percent decrease from maximum $\{[1 - (Q_{obs}/Q_{max})] \times 100\%\}$ was calculated. All titrations were performed in triplicate. Binding affinity was calculated by using the single-site Langmuir binding equation (Kim *et al.*, 1994) and GraphPad Prism 3.0 software.

2.7. Cell Lines and Cell Culture

The MDA-MB-435 human breast carcinoma cell line, which was isolated from a pleural effusion (Schmidt *et al.*, 1999); the DU 145 human prostate carcinoma cell line (American Type Tissue Culture, Manassas, VA), which was isolated from a distal brain metastatic lesion (Mickey *et al.*, 1977); and the LNCaP human prostate cell line (American Type Tissue Culture), which was isolated from a proximal lymph node metastatic lesion (Horoszewicz *et al.*, 1983), were used in these studies. The B16-F1 melanoma cell line (Fidler, 1975) served as a negative control. Cells were grown to confluence in RPMI 1640 media (GIBCO-BRL, Grand Island, NY) supplemented with L-glutamine, 10% fetal bovine serum, sodium pyruvate, and nonessential amino acids.

2.8. Cell Surface Binding and Digital Image Analysis

Dispersed cell suspensions ($2–4 \times 10^6$ cells/ml) were prepared in 1 × phosphate-buffered saline (PBS), pH 7.4, and 4% formaldehyde, as described previously (Peletskaya *et al.*, 1997). One 5-μl drop of each cell suspension was placed on each microscope slide. Slides were dried overnight at room temperature (RT). All peptide incubations were conducted simultaneously under identical conditions. Slides were blocked (10 mM Tris, pH 7.5, 6% BSA) and washed. Slides were incubated with peptide solution (100 μM or 20 μM, 10 mM Tris, pH 7.5, 1% BSA) for 1 hr at RT. When appropriate, peptide solutions were preincubated with 1 mM free TF antigen (Accurate Chemical Co., Westbury, NY) for 1 hr. The slides were washed and blocked, and 10 μg/ml NeutrAvidin-Texas Red (Molecular Probes, Eugene, OR) was added for 1 hr at RT in the dark. Finally, the slides were washed, and mounting media and coverslips were added. The slides were stored in the dark at 4°C until use. Laser scanning confocal microscopy was performed on a Bio-Rad MRC 600 confocal microscope (University of Missouri Molecular Cytology Core Facility).

Mean pixel fluorescence intensity analysis (MPFI) was used to prepare a semiquantitative analysis of fluorescence intensity of peptide binding to cultured carcinoma cell lines (Bains *et al.*, 1997; Hallahan and Virudachalam, 1997; Li *et al.*, 1997; Miller *et al.*, 1997; Millis *et al.*,

1997; Naureckiene *et al.,* 2000). The Adobe Photoshop "Histogram" function reported MPFI in AU (Miller *et al.,* 1997). Prior to statistical analysis, both background noise (the autofluorescence of cell-free areas) (Bour-Dill *et al.,* 2000; Smith and Lange, 2001; Wohland *et al.,* 1999; Zucker and Price, 2001) and biochemical noise (the binding of the peptide to the control B16-F1 cell line) (Bour-Dill *et al.,* 2000; Garini *et al.,* 1999; Zucker and Price, 2001) were subtracted from each individual MPFI value. MPFI is reported numerically as mean MPFI (in AU) ± standard deviation.

2.9. Inhibition of Homotypic Aggregation of Cultured Human Carcinoma Cells

The ability of the second-generation peptides to inhibit TF antigen-mediated homotypic aggregation in the MDA-MB-435 human breast carcinoma cell line, which is a well-established cultured cell model of homotypic aggregation (Glinsky *et al.,* 2000; Glinsky *et al.,* 2001), was determined. These assays were conducted essentially as described in the literature (Lotan and Raz, 1983; Meromsky *et al.,* 1986; Raz and Lotan, 1981; Updyke and Nicolson, 1986). Subconfluent MDA-MB-435 human breast carcinoma cells were suspended and diluted to 2×10^6 cells/ml by using Ca^{2+}- and Mg^{2+}-free Dulbecco's PBS, 2 mM EDTA (CM-DPBS) (GIBCO-BRL) (Lotan and Raz, 1983; Meromsky *et al.,* 1986; Raz and Lotan, 1981; Updyke and Nicolson, 1986). Cell viability was assessed by trypan blue (Sigma Chemical Co.) exclusion assay. The peptide P30-1, which was highly specific for the TF antigen and also exhibited the highest binding intensity to MDA-MB-435 cells, was used to initially define the effect of combinatorial maturation on the ability of the second-generation peptides to inhibit homotypic adhesion of MDA-MB-435 cells. Increasing concentrations of ASF (300 fM to 300 μM) in CM-DPBS were preincubated in the presence or absence of 100 μM P30-1 for 0.5 hr at 37°C in a rotating water bath (75 rpm) in siliconized glass test tubes (Meromsky *et al.,* 1986). Then, 5×10^5 MDA-MB-435 cells were added (final volume = 500 μl), and the reaction was incubated for 1 hr at 37°C. The number of aggregated and single cells in digital fields (×20 magnification) was recorded. Percent aggregation at each ASF concentration was calculated by dividing the number of aggregated cells by the total number of cells (aggregated plus single cells) and multiplying by 100. In the absence of ASF, a low level of spontaneous aggregation was observed, which was not significantly reduced by the addition of 100 μM P30-1. Basal aggregation was subtracted from all observations before analysis to account for this. The concentration of ASF that caused half-maximal aggregation (EC_{50}) was calculated by using sigmoidal nonlinear regression analysis and the GraphPad Prism software package. To compare the inhibition of homotypic aggregation among the second-generation peptides and to compare maturation of this function to that observed for the first-generation peptide P30, 1.5 nM ASF (the EC_{50} concentration) was preincubated in the presence and absence of 100 μM or 20 μM of the second-generation peptides P30-1 or P17, the first-generation-peptide P30, or a nonrelevant control peptide and the homotypic aggregation assay was conducted, as described earlier. Three independent replicates were completed of all experiments. Statistical significance was determined by using an unpaired, one-tailed *t* test and the GraphPad Prism software package.

3. RESULTS AND DISCUSSION

3.1. Combinatorial Affinity Maturation of Anti-TF Antigen Peptides

The TF antigen, when exposed on the surface of carcinoma cells, has been shown to participate in cell adhesion (Glinsky *et al.,* 2000, 2001; Matarrese *et al.,* 2000) and migration (Matarrese *et al.,* 2000) functions that promote metastasis (Fridman *et al.,* 1990; Jessup *et al.,* 1993; Li *et al.,* 2001; Lotan and Raz, 1983; Luzzi *et al.,* 1998; Meromsky *et al.,* 1986; Saiki *et al.,* 1991; Updyke and Nicolson, 1986; Yakushijin *et al.,* 1998). Earlier observations from our laboratory, as well as others, indicated that anti-TF antigen agents, such as antibodies (Wang *et al.,* 1997) and peptides (Glinsky *et al.,* 2000; Glinsky *et al.,* 2001; Peletskaya *et al.,* 1996, 1997), may be valuable in carcinoma diagnosis and could provide valuable insight into the role of the TF antigen in homotypic carcinoma cell aggregation. Previously, we isolated TF antigen–binding peptides by using combinatorial bacteriophage display selection. The peptides bound to the TF antigen on carcinoma cells but were of low affinity and low solubility in physiological buffers. In the present study, we sought improved anti-TF antigen peptides that possessed enhanced carcinoma cell–targeting abilities, potent antimetastatic activities, and increased solubility.

The selection strategy was designed to mimic the strategy of recombination and somatic mutation used by the human immune system to build a repertoire of high-affinity antibodies (Foote and Eisen, 2000). To accomplish this, randomized sequence was combined with a known TF antigen–binding consensus sequence. The selection strategy was designed to expand the sequence space from which to select TF antigen–binding peptides

and to increase the probability of selecting high-affinity binding (Scott and Smith, 1990). Increased stringency (Scott and Smith, 1990) was clearly observed in the decrease in the number of phage eluted during each succeeding round of selection. The yield from each selection round (from 1.0×10^{-2}% to 6.0×10^{-4}%) was significantly above the level of nonspecific absorption (3.5×10^{-5}%) (Scott and Smith, 1990), which indicated that specific affinity selection of TF antigen–binding bacteriophage had occurred (Scott and Smith, 1990).

3.2. Binding of Synthesized Peptides to the TF Antigen on Immobilized Glycoproteins

Analysis of the deduced peptide sequences indicated that the TF antigen–binding consensus sequence was intact in the center of all recombinant peptides. A peptide was selected for synthesis and prospective characterization if the displayed peptide gave a high intensity signal in a bacteriophage membrane binding assay (data not shown) and/or if the deduced peptide sequence was represented with high frequency among the selected bacteriophage clones. Since the first-generation peptides were highly insoluble, the putative physicochemical nature of the peptides was also considered during the choice of peptides for synthesis. Hence, a peptide was selected for synthesis if the analysis of the calculated isoelectric point (pI) and calculated net molecular charge at pH 7.5 (deduced by applying the Henderson-Hasselbach equation) indicated that the peptide might be more water-soluble than the first-generation peptide, P30. Given these guidelines, two peptide sequences were selected for synthesis (Table 1), including P30-1 (IVWHRWYAWSPASRI) and P17 (YYAWHWYAWSPKSV-). These peptides tended to have more basic calculated pI and/or higher calculated net molecular charges than did P30 (data not shown). During the subsequent functional characterization, it was observed that precipitation of the second-generation peptides occurred at 5- to 10-fold higher concentrations (100–500 μM) than for the first-generation peptides (10–50 μM). This indicated that the second-generation peptides were more water soluble in physiological buffers than was P30.

Binding to immobilized ASF was used initially to determine if the synthesized peptides could bind to the TF antigen displayed on ASF (Fig. 1). Detectable signals over background binding (blot with SA-AP only) suggested that the two synthesized second-generation peptides bound to immobilized ASF with detectably higher intensity than did the first-generation peptide P30. The increase in binding intensity was most dramatic for P30-1, which bound with nearly 80% higher intensity than did P30.

Table 1. Sequences and Relative Affinity of Microlibrary Peptides

Name	Sequence	ASFa	Maturation[b]
P30-1	IVWHRWYAWSPASRI	581.1 ± 98.0	0.6
P17	YYAWHWYAWSPKSV-	69.9 ± 19.6	4.6
P30	HGRFILPWWYAFSPS	321.9 ± 70.0	—
Control	RNVPPIFNDVYWIAF	ND[c]	ND[3]

[a] K_d ± SEM, nM.
[b] Maturation = increase in affinity relative to P30. $1/(K_d^{(peptide)}/K_d^{(P30)})$.
[c] ND, no detectable binding.

3.3. Binding Affinity of Synthesized Peptides to the TF Antigen on Glycoproteins

To analyze binding affinity more accurately and precisely, a solution binding assay, fluorescence quenching, was used to calculate the dissociation constant (K_d) that described binding affinity. Binding of the peptides to the TF antigen displayed on ASF was detected by observing a quenching of AlexaFluor 488 fluorescence. Initial spectral analyses indicated that the two second-generation peptides P30-1 and P17 caused significant quenching of AlexaFluor 488 fluorescence at a wavelength of 519 nm. The maximal quenching that resulted from binding of 10 μM P30-1 to labeled ASF was more than twice that observed for the same concentration of the first-generation peptide, P30 (Fig. 2). P17 (10 μM) also caused a larger magnitude of quenching than did P30 (data not shown). A 10-fold higher concentration of

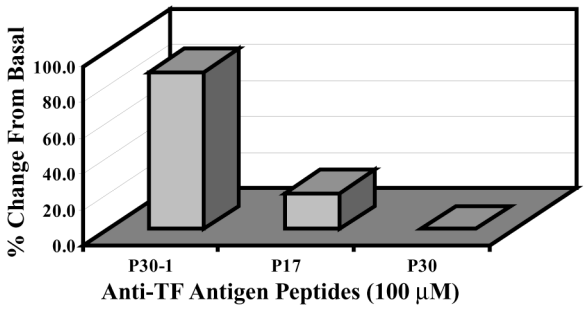

Fig. 1. Binding of anti-TF antigen peptides to TF antigen displayed on immobilized ASF. The 1-μL dots of 1 mM ASF or buffer only were spotted onto nitrocellulose and dried. The membranes were incubated with biotinylated anti-TF antigen peptides (100 μM), control peptide (100 μM), or SA-AP only and developed colorimetrically. Blots were scanned and intensity of binding was analyzed, as described in "Materials and Methods." The data are presented as percent change from basal with the MPI of P30 being designated as basal MPI.

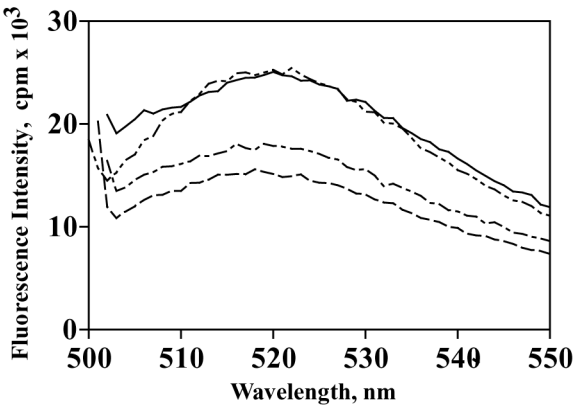

Fig. 2. Quenching of AlexaFluor 488 fluorescence by anti-TF antigen peptides. ASF (1 nM) was covalently labeled with AlexaFluor 488. Binding of anti-TF antigen peptides (10 μM), but not the control peptide (100 μM), to the TF antigen displayed on ASF quenches AlexaFluor 488 fluorescence. Representative emission scans are shown for 1 nM ASF alone (solid line), 1 nM ASF plus 10 μM 30-1 (— —), 1 nM ASF plus 10 μM P30 (— – —), and 1 nM ASF plus 100 μM control peptide (— – – —). The percent quenching by peptides relative to the cognate unliganded ASF solution at 519-nm wavelength was calculated. P30-1, 43.0%; P30, 27.3%; control peptide, <0.01%.

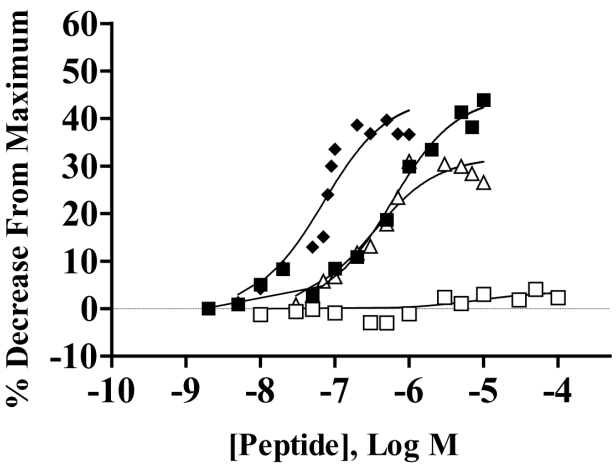

Fig. 3. Affinity of binding to the TF antigen by affinity maturated anti-TF antigen peptides. ASF was covalently labeled with AlexaFluor 488. Binding of anti-TF antigen peptides to the TF antigen displayed on ASF quenches AlexaFluor 488 fluorescence in a dose-dependent manner. P30-1 (filled squares), K_d = 581.1 ± 98.0 nM; P17 (filled diamonds), K_d = 69.9 ± 19.6 nM; P30 (open triangles) K_d = 321.9 ± 70.0 nM; P-Control (open squares, RNVPPIFNDVYWIAF), K_d = not calculated. Affinity (K_d) was calculated by using the Langmuir binding equation and was reported as K_d ± SEM. Error bars were eliminated for clarity.

the control peptide resulted in no quenching, which indicated that the control peptide did not bind to ASF.

Fluorescence quenching titrations were conducted to observe the dose-dependent quenching of AlexaFluor 488 fluorescence and to derive K_d values for binding affinity (Kim *et al.*, 1994) (Fig. 3). Both of the synthesized second-generation peptides bound with detectable affinity to the TF antigen displayed on ASF. As peptide monomers, the second-generation peptide P17 exhibited a greater than fivefold increase in affinity ($K_d \cong 60$ nM) over the affinity of the best characterized of the first-generation peptides (P30, K_d = 320 nM) for the TF antigen (Fig. 3). P30-1 did not show an increase in affinity (K_d = 581.1 ± 98.0 nM) relative to P30. Binding to the TF antigen was saturable and the change from 10% saturation to 90% saturation occurred over an approximately 100-fold concentration range, which indicated a specific single-site, noncooperative binding event.

Although the increase in affinity was not enormous, it is consistent with reports of the degree of affinity maturation achieved in carbohydrate binding antibodies, which are much larger proteins. Yelton *et al.* (1995) reported a 5- to 15-fold increase in binding affinity after *in vitro* maturation of a Fab fragment of an anti-carbohydrate antibody and a 65-fold increase for the complete IgG molecule. Additional increases in affinity for anti-TF antigen peptides may be achieved by using multiple antigenic peptide (MAP) multimeric constructs.

3.4. Binding of Peptides to the TF Antigen Displayed on the Surface of Cultured Carcinoma Cells

Because the anti-TF antigen peptides were selected against immobilized, purified glycoproteins, we asked if the isolated peptides would specifically recognize the TF antigen displayed in the context of a cell surface and if the observed differences in the affinity of peptide binding to the TF antigen presented on ASF would translate into differential binding to the surfaces of cultured carcinoma cells. Previously, the first-generation peptide P30 was shown to bind at high concentrations (100 μM) to the TF antigen exposed on the surface of cultured human breast carcinoma cells (Glinsky *et al.*, 2000, 2001; Peletskaya *et al.*, 1997). To compare the binding of the maturated peptides with that of the first-generation peptides, we observed binding to the MDA-MB-435 human breast carcinoma cell line (Schmidt *et al.*, 1999) used in the original P30 studies. Additionally, two cultured human prostate carcinoma lines (DU 145 and LNCaP), which were derived from different metastatic stages (Horoszewicz *et al.*, 1983; Mickey *et al.*, 1977), were used. At high concentration (100 μM), both second-generation peptides (P30-1, P17) and the first-generation peptide P30 bound with high intensity to the surfaces of cultured human breast and prostate carcinoma cell lines (data not shown). There was no binding by anti-TF antigen peptides to the TF antigen-negative control cell line, B16-F1.

If our hypothesis was correct, we expected to see an improvement in the cell surface binding characteristics of the second-generation peptides relative to P30. However, the saturating intensity of high-concentration binding indicated that a lower peptide concentration was required to answer the question posed. In fluorescence quenching titrations, saturated binding was achieved by the second-generation peptides at a concentration of 20 μM. When the cell surface binding experiments were repeated with this lower peptide concentration (20 μM), virtually no binding of the first-generation peptide P30 to the TF antigen displayed on cultured carcinoma cell surfaces was visible, with the exception of low-intensity binding to the human prostate carcinoma cell line DU 145 (Fig. 4). This differential binding suggested that the level of exposure of the TF antigen might differ between the carcinoma cell lines. A control experiment, which was conducted to observe the binding of the TF antigen–

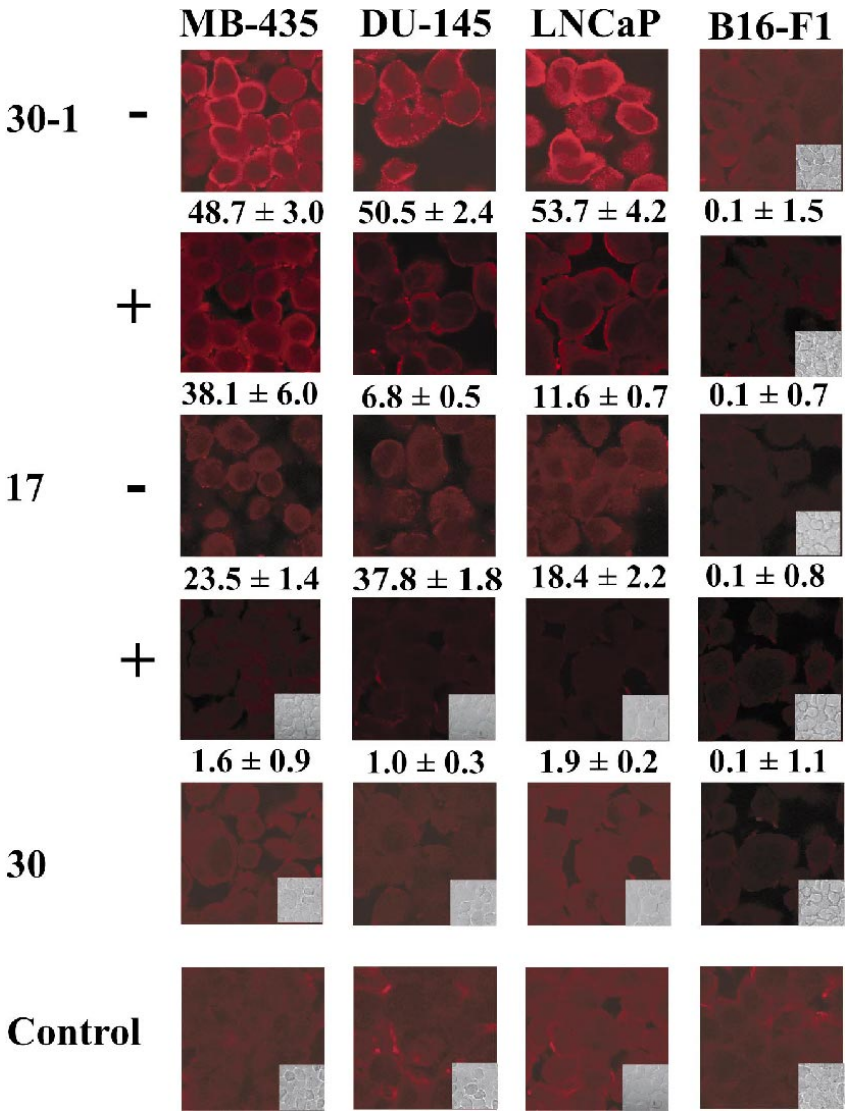

Fig. 4. Binding of anti-TF antigen peptides to TF antigen displayed on cultured carcinoma cells. Laser scanning confocal microscopic examination of cell surface binding of P30-1 and P17 (20 μM) in the presence (+) and absence (−) of competitor (1 mM free TF antigen) and MPFI analysis were conducted, as described in "Material and Methods." Binding of P30 and a nonrelevant control peptide are shown for comparison. Fold reduction in binding intensity to the prostate lines was calculated by dividing the MPFI in the absence of free TF antigen by the MPFI in the presence of free TF antigen. The fold reduction in binding intensity to DU 145 cells was 7.4 and 19.9 for P30-1 and P17, respectively. The fold reduction in binding intensity to LNCaP cells was 4.6 and 18.4 for P30-1 and P17, respectively.

specific peanut (*Arachis hypogaea*) lectin (PNA) (Lotan *et al.,* 1975) to carcinoma cell surfaces, suggested that the low-intensity binding of P30 to the surface of DU 145 cells resulted from the concentration of the TF antigen on the cell surface as opposed to the dispersed binding sites in the other cell lines (data not shown).

Visual analysis indicated that the second-generation peptides (20 μM) P30-1 and P17 (Fig. 4) bound with higher intensity to the TF antigen displayed on carcinoma cell surfaces than did P30. These three peptides showed no visibly detectable binding to the negative control cell line, B16-F1. Visual evaluation suggested that P30-1 bound with higher intensity to the panel of cell lines than did P17. Both peptides also showed diffuse, low-intensity binding within the cytoplasm of the carcinoma cells.

To confirm our visual observation of differing intensity binding by peptides, a semiquantitative digital analysis of peptide binding to the cell surface TF antigen was conducted. Similar semiquantitative image analyses have been applied in plant (Li *et al.,* 1997) and mammalian cells (Hallahan and Virudachalam, 1997) to protein expression (Bains *et al.,* 1997; Millis *et al.,* 1997) and cellular transport functions (Miller *et al.,* 1997; Millis *et al.,* 1997). The relative differences in binding intensity detected during the MPFI analysis represented real differences in binding, since two sources of nonspecific signal were removed before analysis and stringent technical controls were applied to reduce variability between the digital images to allow relative comparisons of binding intensity. In cell surface binding assays, MPFI analysis clearly showed an increase in signal intensity for P30-1 and P17 relative to the first-generation peptide, P30 (Fig. 4). The digital image analysis confirmed our visual analysis that P30-1 bound with higher intensity to all cell lines than did P17.

3.5. Specificity of Carbohydrate Binding

The effects of affinity maturation on the specificity of carbohydrate binding by the second-generation peptides was defined. While, for the most part, *in vitro* maturation of affinity has not been reported to affect the molecular determinants of the specificity of binding (Yelton *et al.,* 1995), intentional broadening of binding specificity via functional maturation has been reported for some proteins, including cytokines (Chang *et al.,* 1999) and antibodies (Barbas *et al.,* 1994).

In this study, combinatorial affinity maturation appeared to result in increased binding specificity for the TF antigen over closely related carbohydrates. The first hint of a change in specificity was the differential competition by 1 mM free TF antigen for binding of P17 and P30-1 to cell surface TF antigen in the DU 145 and LNCaP prostate carcinoma cell lines (Fig. 4). To assess specificity of peptide binding to cell surface carbohydrates, biotinylated peptides were preincubated with free TF antigen. Cell surface binding was observed by using laser scanning confocal microscopy. While there was competition by 1 mM free TF antigen for binding of both second-generation peptides (20 μM) to all cell lines, strikingly different degrees of competition by free TF antigen were observed for the binding of P17 and P30-1 to the two prostate lines (Fig. 4). Both visual and MPFI analyses indicated that the free TF antigen competed with high efficiency for P17 binding to both LNCaP cells (1.0 ± 0.3 AU) and DU 145 cells (1.9 ± 0.2 AU). In contrast, the free TF antigen was unable to completely compete (a sixfold reduction in MPFI) for P30-1 binding to either LNCaP (11.6 ± 0.7 AU) or DU 145 (6.8 ± 0.5 AU). Thus, P17 appeared to be more specific for cell surface TF antigen than was P30-1. There was no competition by 1 mM free TF antigen for binding of P30 or the control peptide to any of the three cultured human carcinoma cell lines (data not shown).

Subsequent fluorescence quenching titrations, which were conducted to define the difference in specificity in an *in vitro* system and to derive K_d values to describe the affinity of peptide binding to related oligosaccharides (Fig. 5), indicated that both second-generation peptides had evolved greater specificity for the TF antigen than that possessed by the first-generation peptide, P30. Transferrin, which displays sialyl-galactose β1→4 *N*-acetylglucoseamine (sialyl-LACNAc) (Finne and Krusius, 1979), and fetuin, which displays the sialylated-TF antigen (Edge and Spiro, 1987), were labeled with AlexaFluor 488 and used as fluorophores. Both P30-1 (Fig. 5A) and P17 (Fig. 5B) possessed reduced affinity for sialyl-LACNAc (P30-1, $K_d = 13.3 \pm 3.2$ μM, 27-fold reduction; P17, $K_d = 379.1 \pm 94.1$ nM, 18-fold reduction) compared with the TF antigen. Both peptides also bound with very low affinity to the sialyl-TF antigen displayed on fetuin (data not shown). Finally, the affinities of the second-generation peptides for the different carbohydrates were compared with those of P30. P30 (Fig. 5C) bound to sialyl-LACNAc ($K_d = 1.1 \pm 0.15$ μM.) with 3.4-fold lower affinity than to the TF antigen ($K_d = 321.9 \pm 70$ nM). Therefore, affinity maturation appears to have also resulted in selection of second-generation peptides (P17 and P30-1) with higher specificity for the TF antigen compared with the first-generation peptide P30.

3.6. Inhibition by Anti-TF Antigen Peptides of Homotypic Aggregation of Cultured Human Carcinoma Cells

Experiments were conducted to determine if, in addition to maturation of the anti-TF antigen peptides'

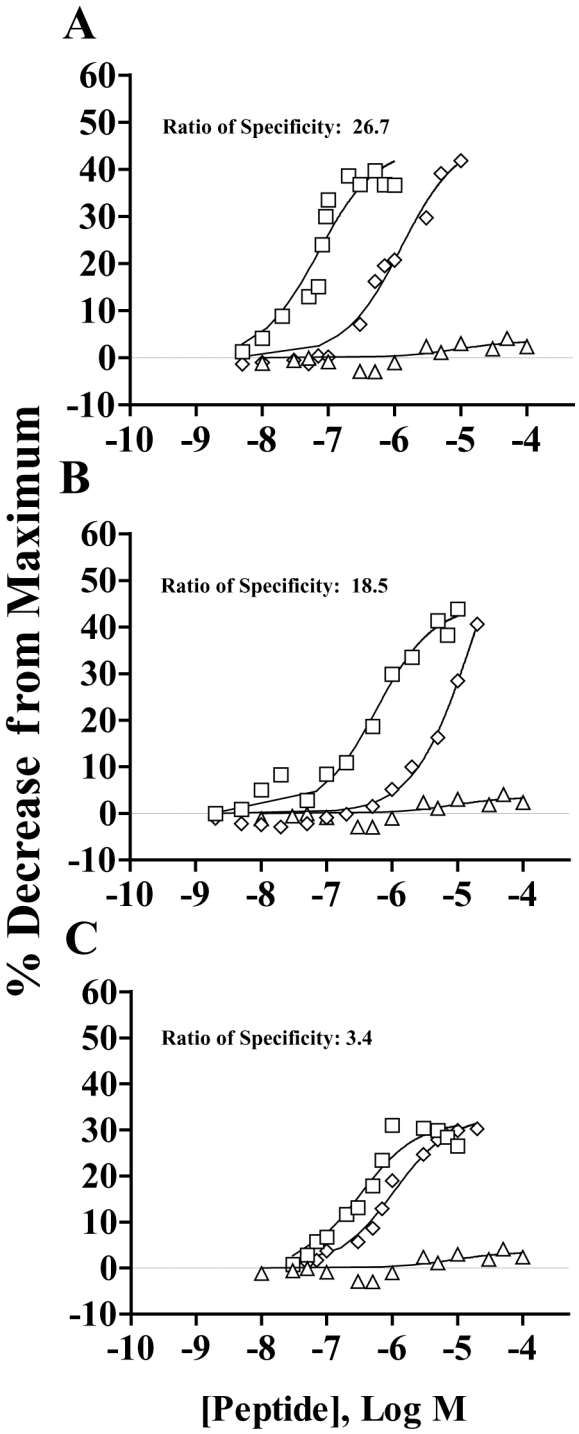

Fig. 5. Specificity of binding by second-generation peptides P30-2 and P17. Fluorescence quenching titrations of binding of P30-1 (**A**), P17 (**B**), and P30 (**C**) to AlexaFluor 488–labeled ASF (filled squares) and transferrin (filled diamonds) was conducted, as described in "Materials and Methods." Binding of the control peptide to AlexaFluor 488–labeled ASF (filled triangles) is shown for comparison. The ratio of specificity was calculated by dividing the K_d describing affinity of peptide binding to labeled transferrin by the K_d describing affinity of binding to labeled ASF. Affinities of the peptides for the transferrin disaccharide are (**A**) P30-1, $K_d = 15.6 \pm 4.1$ μM; (**B**) P17, $K_d = 1.3 \pm 0.2$ μM; and (**C**) P30, $K_d = 1.1 \pm 0.1$ μM. In all parts, affinity (K_d) was calculated by using the Langmuir binding equation and was reported as $K_d \pm$ SEM. Error bars were eliminated for clarity.

binding affinity and specificity, maturation of a physiologically relevant function had occurred. We chose to observe the effect of combinatorial maturation on the peptides' abilities to inhibit homotypic aggregation of carcinoma cells because the link between TF antigen–mediated carcinoma cell homotypic adhesion and metastatic potential has been amply demonstrated in a number of tumorigenic cell lines. Thus, if the maturated anti-TF antigen peptides could reduce TF antigen–mediated homotypic aggregation, they might have important clinical applications in reducing the metastatic potential of carcinoma cells (Fig. 6).

The prospective physiological and clinical importance of the second-generation peptides was demonstrated by the enhanced ability of the second-generation peptides, compared with the first generation peptides, to inhibit metastasis-related homotypic adhesion. The best and most widely used *in vitro* assay for TF antigen–mediated adhesion in carcinoma cells is ASF-stimulated homotypic adhesion. Previously, our laboratory demonstrated that the first-generation peptide P30 inhibited homotypic adhesion in MDA-MB-435 human breast carcinoma cells, presumably by binding to and occluding the TF antigen (Glinsky *et al.*, 2000, 2001). The second-generation peptide P30-1, which was highly specific for the TF antigen and also exhibited the highest binding intensity to MDA-MB-435 cells, was used to initially define the effect of combinatorial maturation on the ability of the second-generation peptides to inhibit homotypic adhesion of MDA-MB-435 cells (viability >95%).

In our hands, the TF antigen, which was presented on ASF, mediated homotypic adhesion of MDA-MB-435 cells, which was significantly inhibited by the maturated anti-TF antigen peptides. Addition of ASF to a single-cell suspension of cultured MDA-MB-435 cells induced a dose-dependent increase in homotypic aggregation (Fig. 5A). The ASF concentration causing half-maximal aggregation was determined by nonlinear regression to be approximately 1.5 nM ASF (Fig. 5A). By binding to the TF antigen and occluding its interaction with cell surface lectins, P30-1 (100 μM) reduced the potency of ASF-induced aggregation by nearly 1000-fold, with half-maximal aggregation occurring at an ASF concentration of 1.6 μM (Fig. 5A). To compare differences in inhibition of TF antigen–mediated homotypic aggregation among the second-generation peptides and relative to the first-generation peptide P30, 1.5 nM ASF (the EC_{50} concentration) was preincubated with anti-TF antigen pep-

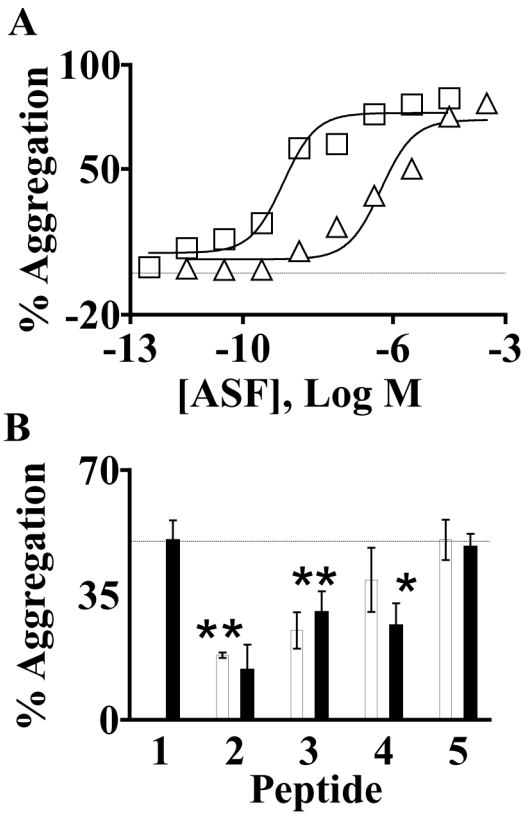

Fig. 6. Inhibition of homotypic adhesion by second-generation anti-TF antigen peptides. (**A**) The percentage homotypic aggregation of MDA-MB-435 cells in the presence of increasing concentrations of ASF (open squares) and in the presence of 100 μM P30-1 (open triangles) was calculated, as described in "Material and Methods." The effective concentration at which 50% homotypic adhesion occurred (EC_{50}) was calculated by using sigmoidal dose–response nonlinear regression and GraphPad Prism software and was reported as $EC_{50} \pm$ SEM (ASF in the absence of P30-1, $EC_{50} = 1.5 \pm 0.48$ nM; ASF in the presence of 100 μM P30-1, $EC_{50} = 1.6 \pm 1.2$ μM). Error bars were eliminated for clarity. (**B**) Inhibition of homotypic aggregation of MDA-MB-435 cells stimulated by 1.5 nM ASF in the absence of peptide (shaded bar, #1), or in the presence of 100 μM peptide (shaded bars) or 20 μM peptide (open bars). The numbers below the x-axis denote the conditions (#1 = 1.5 nM ASF minus peptide, #2 = 1.5 nM ASF plus P30-1, #3 = 1.5 nM ASF plus P17, #4 = 1.5 nM ASF plus P30, #5 = 1.5 nM ASF plus nonrelevant control peptide). Conditions in which the mean inhibition of aggregation by an anti-TF antigen peptide significantly differs ($P < 0.05$) from the control condition (1.5 nM ASF, "-Pep") are denoted by asterisks (*). Statistical significance was determined by using a one-tailed, unpaired *t* test and the GraphPad Prism software package.

tides (100 μM or 20 μM) before incubation with MDA-MB-435 cells and inhibition of aggregation was observed. At a concentration of 100 μM, both the second-generation peptides and the parental peptide P30 were able to significantly reduce homotypic aggregation of MDA-MB-435 cells (Fig. 5B). At 100 μM, P30-1 caused a greater inhibition of aggregation than did either the first-generation peptide P30 or the second-generation peptide P17. However, when the concentration of the peptides was reduced to 20 μM (Fig. 5B), it became apparent the second-generation peptides P30-1 and P17 more effectively inhibited aggregation than did the first-generation peptide P30. At 20 μM, the maturated anti-TF antigen peptides were able to effect a statistically significant reduction in ASF-mediated homotypic aggregation. In contrast, the first-generation peptide P30 produced only a slight decrease in aggregation, which was not statistically significant. At a peptide concentration of 20 μM, P30-1 was more effective than either P17 or P30, but P17 caused a much greater reduction in inhibition than did P30. The inhibition of aggregation caused by the second-generation anti-TF antigen peptides did not appear to be a nonspecific effect of the presence of the peptides in the system because a nonrelevant control peptide did not reduce ASF-mediated homotypic aggregation at either concentration. These observations also indicated that the second-generation peptides might inhibit metastasis-related processes at physiologically significant concentrations, perhaps down into the nM range and that anti-TF antigen peptides can substantially reverse aggregation, even at very low TF antigen concentrations.

ASF, which has been classically used to induce TF antigen–mediated homotypic aggregation (Glinsky *et al.*, 2000, 2001; Inohara and Raz, 1995; Lotan and Raz, 1983; Meromsky *et al.*, 1986), displays three copies of the *N*-linked *N*-acetyl-lactosamine disaccharide in addition to three TF antigen molecules. Although the magnitude of inhibition by the second-generation anti-TF antigen peptides indicates that the TF antigen plays the primary role in mediating homotypic aggregation, future experiments will be conducted to further clarify the individual role of the TF antigen and the anti-TF antigen peptides in homotypic aggregation by using the TF antigen, which is covalently conjugated to HSA, in the presence and absence of anti-TF antigen peptides.

Nevertheless, our data clearly showed that the second-generation peptides could inhibit homotypic aggregation and strongly suggests that the maturated peptides may have an important clinical application as antiadhesive, and possibly antimetastatic, agents. Combinatorial maturation of function resulted in the second-generation peptides that were able to inhibit aggregation at a low peptide concentration, at which no inhibition by the first-generation peptide P30 was detected. Future experiments will be conducted to clarify the prospective role of the second-generation peptides in decreasing metastatic potential, including observing inhibition of aggregation by MAP constructs and determining the cell line and tumor-type dependence of inhibition of aggregation by the second-generation peptides. There are a multiplicity

of clinical and basic science applications for the second-generation anti-TF antigen peptides, offering exciting prospects for increasing the understanding of the role of the TF antigen, as well as carbohydrates in general, in the development and progression of carcinoma.

ACKNOWLEDGMENTS

Cultured carcinoma cell lines were kindly provided by researchers Dr. J. E. Price (MDA-MB-435) and Dr. I. J. Fidler (B16-F1, LNCaP). The authors would like to thank Marie Dickerson for technical assistance; Dr. Olga Glinskii for cell culture; the University of Missouri Molecular Cytology core facility for assistance in laser scanning confocal microscopy; Dr. George Smith for invaluable advice regarding bacteriophage display technique and analysis; Dr. Fabio Gallazzi for synthesizing the peptides; and Drs. Andrey Komissarov, Peter Tipton, and Michael Henzl for assistance with fluorescence quenching.

REFERENCES

Bains, R., Furness, P. N., and Critchley, D. R. (1997). *J. Pathol.* **183:** 272–280.
Baldus, S. E., Hanisch, F. G., Kotlarek, G. M., Zirbes, T. K., Thiele, J., Isenberg, J., *et al.* (1998). *Cancer* **82:** 1019–1027.
Baldus, S. E., Zirbes, T. K., Hanisch, F. G., Kunze, D., Shafizadeh, S. T., Nolden, S., *et al.* (2000). *Cancer* **88:** 1536–1543.
Barbas, C. F., 3rd, Hu, D., Dunlop, N., Sawyer, L., Cababa, D., Hendry, R. M., *et al.* (1994). *Proc. Natl. Acad. Sci. USA* **91:** 3809–3813.
Bour-Dill, C., Gramain, M. P., Merlin, J. L., Marchal, S., and Guillemin, F. (2000). *Cytometry* **39:** 16–25.
Brockhausen, I., Schutzbach, J., and Kuhns, W. (1998). *Acta Anat. (Basel)* **161:** 36–78.
Cao, Y., Stosiek, P., Springer, G. F., and Karsten, U. (1996). *Histochem. Cell Biol.* **106:** 197–207.
Chang, C. C., Chen, T. T., Cox, B. W., Dawes, G. N., Stemmer, W. P., Punnonen, J., *et al.* (1999). *Nat. Biotechnol.* **17:** 793–797.
De Kroon, A. I., Soekarjo, M. W., De Gier, J., and De Kruijff, B. (1990). *Biochemistry* **29:** 8229–8240.
Edge, A. S., and Spiro, R. G. (1987). *J. Biol. Chem.* **262:** 16135–16141.
Fidler, I. J. (1975). *Cancer Res.* **35:** 218–224.
Finne, J., and Krusius, T. (1979). *Eur. J. Biochem.* **102:** 583–588.
Foote, J., and Eisen, H. N. (2000). *Proc. Natl. Acad. Sci. USA* **97:** 10679–10681.
Fridman, R., Giaccone, G., Kanemoto, T., Martin, G. R., Gazdar, A. F., and Mulshine, J. L. (1990). *Proc. Natl. Acad. Sci. USA* **87:** 6698–6702.
Garini, Y., Gil, A., Bar-Am, I., Cabib, D., and Katzir, N. (1999). *Cytometry* **35:** 214–226.
Glinsky, V. V., Glinsky, G. V., Rittenhouse-Olson, K., Huflejt, M. E., Glinskii, O. V., Deutscher, S. L., *et al.* (2001). *Cancer Res.* **61:** 4851–4857.
Glinsky, V. V., Huflejt, M. E., Glinsky, G. V., Deutscher, S. L., and Quinn, T. P. (2000). *Cancer Res.* **60:** 2584–2588.
Hallahan, D. E., and Virudachalam, S. (1997). *Proc. Natl. Acad. Sci. USA* **94:** 6432–6437.
Horoszewicz, J. S., Leong, S. S., Kawinski, E., Karr, J. P., Rosenthal, H., Chu, T. M., *et al.* (1983). *Cancer Res.* **43:** 1809–1818.
Inohara, H., and Raz, A. (1995). *Cancer Res.* **55:** 3267–3271.
Jain, R. K. (1989). *J. Natl. Cancer Inst.* **81:** 570–576.
Jessup, J. M., Petrick, A. T., Toth, C. A., Ford, R., Meterissian, S., O'Hara, C. J., *et al.* (1993). *Br. J. Cancer* **67:** 464–470.
Kim, C., Paulus, B. F., and Wold, M. S. (1994). *Biochemistry* **33:** 14197–14206.
Komissarov, A. A., Calcutt, M. J., Marchbank, M. T., Peletskaya, E. N., and Deutsher, S. L. (1996). *J. Biol. Chem.* **271:** 12241–12246.
Komissarov, A. A., Marchbank, M. T., Calcutt, M. J., Quinn, T. P., and Deutscher, S. L. (1997). *J. Biol. Chem.* **272:** 26864–26870.
Li, G., Satyamoorthy, K., and Herlyn, M. (2001). *Cancer Res.* **61:** 3819–3825.
Li, S., Spear, R. N., and Andrews, J. H. (1997). *Appl. Environ. Microbiol.* **63:** 3261–3267.
Lotan, R., and Raz, A. (1983). *Cancer Res.* **43:** 2088–2093.
Lotan, R., Skutelsky, E., Danon, D., and Sharon, N. (1975). *J. Biol. Chem.* **250:** 8518–8523.
Lundquist, J. J., Debenham, S. D., and Toone, E. J. (2000). *J. Org. Chem.* **65:** 8245–8250.
Luzzi, K. J., MacDonald, I. C., Schmidt, E. E., Kerkvliet, N., Morris, V. L., Chambers, A. F., *et al.* (1998). *Am. J. Pathol.* **153:** 865–873.
Matarrese, P., Fusco, O., Tinari, N., Natoli, C., Liu, F. T., Semeraro, M. L., *et al.* (2000). *Int. J. Cancer* **85:** 545–554.
Meromsky, L., Lotan, R., and Raz, A. (1986). *Cancer Res.* **46:** 5270–5275.
Mickey, D. D., Stone, K. R., Wunderli, H., Mickey, G. H., Vollmer, R. T., and Paulson, D. F. (1977). *Cancer Res.* **37:** 4049–4058.
Miller, D. S., Fricker, G., and Drewe, J. (1997). *J. Pharmacol. Exp. Ther.* **282:** 440–444.
Millis, K. K., Lesko, S. A., and Gamcsik, M. P. (1997). *Cancer Chemother. Pharmacol.* **40:** 101–111.
Mummert, M. E., and Voss, E. W. (1996). *Mol. Immunol.* **33:** 1067–1077.
Naureckiene, S., Sleat, D. E., Lackland, H., Fensom, A., Vanier, M. T., Wattiaux, R., *et al.* (2000). *Science* **290:** 2298–2301.
Panchuk-Voloshina, N., Haugland, R. P., Bishop-Stewart, J., Bhalgat, M. K., Millard, P. J., Mao, F., *et al.* (1999). *J. Histochem. Cytochem.* **47:** 1179–1188.
Peletskaya, E. N., Glinsky, G., Deutscher, S. L., and Quinn, T. P. (1996). *Mol. Divers.* **2:** 13–18.
Peletskaya, E. N., Glinsky, V. V., Glinsky, G. V., Deutscher, S. L., and Quinn, T. P. (1997). *J. Mol. Biol.* **270:** 374–384.
Raz, A., and Lotan, R. (1981). *Cancer Res.* **41:** 3642–3647.
Saiki, I., Naito, S., Yoneda, J., Azuma, I., Price, J. E., and Fidler, I. J. (1991). *Clin. Exp. Metastasis* **9:** 551–566.
Schmidt, C. M., Settle, S. L., Keene, J. L., Westlin, W. F., Nickols, G. A., and Griggs, D. W. (1999). *Clin. Exp. Metastasis* **17:** 537–544.
Scott, J. K., and Smith, G. P. (1990). *Science* **249:** 386–390.
Smith, R. C., and Lange, R. C. (2001). *Crit. Rev. Diagn. Imaging* **42:** 135–140.
Springer, G. F. (1984). *Science* **224:** 1198–1206.
Springer, G. F., Cheingsong-Popov, R., Schirrmacher, V., Desai, P. R., and Tegtmeyer, H. (1983). *J. Biol. Chem.* **258:** 5702–5706.
Springer, G. F., and Desai, P. R. (1977). *Transplant. Proc.* **9:** 1105–1111.
Springer, G. F., Desai, P. R., and Banatwala, I. (1975). *J. Natl. Cancer Inst.* **54:** 335–339.
Updyke, T. V., and Nicolson, G. L. (1986). *Clin. Exp. Metastasis* **4:** 273–284.
Wang, B. L., Springer, G. F., and Carlstedt, S. C. (1997). *J. Histochem. Cytochem.* **45:** 1393–1400.
Wohland, T., Friedrich, K., Hovius, R., and Vogel, H. (1999). *Biochemistry* **38:** 8671–8681.
Yakushijin, Y., Steckel, J., Kharbanda, S., Hasserjian, R., Neuberg, D., Jiang, W., *et al.* (1998). *Blood* **91:** 4282–4291.
Yelton, D. E., Rosok, M. J., Cruz, G., Cosand, W. L., Bajorath, J., Hellstrom, I., *et al.* (1995). *J. Immunol.* **155:** 1994–2004.
Yu, J., and Smith, G. P. (1996). *Methods Enzymol.* **267:** 3–27.
Zucker, R. M., and Price, O. (2001). *Cytometry* **44:** 273–294.